Journal of Solid State Chemistry **166,** 67–72 (2002)
doi:10.1006/jssc.2002.9560, available online at http://www.idealibrary.com on IDEAL®

Crystal Structure of a Lithium Ion-Conducting Perovskite $La_{2/3-x}Li_{3x}TiO_3$ ($x = 0.05$)

Yoshiyuki Inaguma,*[,1] Tetsuhiro Katsumata,* Mitsuru Itoh,† and Yukio Morii‡

* *Department of Chemistry, Faculty of Science, Gakushuin University, 1-5-1 Mejiro, Toshima-ku, Tokyo 171-8588, Japan;* † *Materials and Structures Laboratory, Tokyo Institute of Technology, 4259 Nagatsuta, Midori-ku, Yokohama 226-8503, Japan; and* ‡ *Japan Atomic Energy Research Institute, Tokai-mura, Naka-gun, Ibaraki 319-1195, Japan*

Received November 1, 2001

The crystal structure of a lithium ion-conducting perovskite $La_{0.62(2)}Li_{0.16(1)}TiO_{3.01(3)}$ obtained by furnace-cooling was refined by the Rietveld method using neutron-diffraction data at room temperature and 77 K. The adopted space group was *Cmmm* (No. 65). The anti-phased tilts of TiO_6 octahedra along the *b*-axis in addition to alternative arrangement of La ions along the *c*-axis was confirmed. The position of Li was refined to be off-centered and in two equivalent positions in an A-site. The obtained structural information implies that the lithium ion conduction among A-sites occurs in the vicinity of La-poor layers two-dimensionally rather than three-dimensionally in this compound.

INTRODUCTION

Much attention has been recently paid to lithium ion-conducting perovskites (ABO_3) first reported by Latie *et al.* (1) and Belous *et al.* (2), due to their high conductivity, as a perovskite lanthanum lithium titanate has been found to show lithium ion conductivity as high as $10^{-3}\,S\,cm^{-1}$ at room temperature (3). Though much research has been carried out and the physical properties, structures, and the relations of these compounds are now well known, there are still some controversies, especially over the crystal structure of $La_{2/3-x}Li_{3x}TiO_3$.

Almost all of the proposed atomic models of $La_{2/3-x}Li_{3x}TiO_3$ involve the following: (a) the ordered distribution of La ions on the perovskite A-sites along the *c*-axis, which doubles the cell parameter *c* (4), and (b) unit cells with tetragonal symmetry for the composition with higher Li content ($0.06 < x < 0.14$), and with orthorhombic symmetry for the composition with lower Li content ($x < 0.06$) (5–11).

With respect to the tetragonal phases, two different types of cells have been proposed. One is the cell with $a_p \times a_p \times c(\sim 2a_p)$, where a_p corresponds to the ideal cubic cell parameter, with the space group $P4/mmm$ (5–9). The other is the cell with $2^{1/2}\,a_p \times 2^{1/2}\,a_p \times c(\sim 2a_p)$ proposed by Várez *et al.* (11). With respect to the orthorhombic phases, however, only one type of cell with $a(\sim a_p) \times b(\sim a_p) \times c(\sim 2a_p)$ (space group: *Pmmm*) has been proposed (5, 7, 9, 10).

The degree of ordered distribution of La ions decreases with increases in the Li content (increase in *x*) or temperature (7, 9, 12). The distribution of La ions strongly influences the ionic conductivity because conduction of the Li ions occurs via vacancies and is percolation-controlled by La ions as obstacles in the A-site subcell (13). In fact, a difference in ionic conductivity between the furnace-cooled or annealed samples with the higher degree of order and the quenched sample with the lower degree of order in $La_{2/3-x}Li_{3x}TiO_3$ has been observed (12, 14). In particular, in the vicinity of $x = 0.05$ for $La_{2/3-x}Li_{3x}TiO_3$, the conductivity at 300 K of the furnace-cooled sample is approximately three times higher than that of the quenched sample.

Furthermore, the Li location is one of most important information with regard to elucidating the ion-conduction mechanism. Skakle *et al.* (15) have investigated the crystal structure of $Li_{0.5-3y}Re_{0.5+y}TiO_3$ (Re = Pr, Nd; $y = 0.05$) by neutron diffraction and have reported that it possesses a $GdFeO_3$ structure characterized by the tilts of the TiO_6 and Li ions being located off-center away from the A-site. In contrast, Ruiz *et al.* (8) have structurally characterized tetragonal $La_{0.56}Li_{0.31}TiO_3$ ($x = 0.1$ for $La_{2/3-x}Li_{3x}TiO_3$) by neutron diffraction and have proposed that the Li ions are located at the centre of the A-site at the same position as La.

In this study we chose an orthorhombic perovskite, $La_{2/3-x}Li_{3x}TiO_3$ ($x = 0.05$), obtained by furnace-cooling and investigated the crystal structure with a neutron-diffraction experiment. Based on the crystal data, the

[1] To whom correspondence should be addressed. Fax: + 81-3-5992-1029. E-mail: yoshiyuki.inaguma@gakushuin.ac.jp.

0022-4596/02 $35.00

relation between the structure and the ionic conduction is discussed.

EXPERIMENTAL

The sample was synthesized by a conventional solid-state reaction. The starting materials were La_2O_3(4N), enriched $^7Li_2CO_3$(3N), and TiO_2(3N). The metal content of La_2O_3 was determined by chelatometry with EDTA (ethylenediaminetetraacetic acid). A mixture of the raw materials (the molar ratio of metals was La : Li : Ti = 0.6 : 0.2 : 1) was calcined at 800°C for 4 h, 1150°C for 28 h, and 1250°C for 12 h in air with intermediate grindings. The calcined powder was pressed into pellets and sintered at 1350°C for 6h in air and then furnace-cooled. The pellets were ground and used for the powder X-ray and neutron-diffraction experiments. The molar ratio of the metals for the sample was determined by inductive coupled plasma (ICP) spectroscopy using a SEIKO SPS1500 instrument. The sample was then dissolved as follows. A small amount of sample (about 10 mg) and 1 mL conc. HCl (35 wt%) were sealed in a Pyrex glass tube and kept at approximately 130°C for approximately 10 h in an oven.

The phase was first checked by the powder X-ray diffraction method using a Mac Science MXP18 diffractometer (graphite-monochromatized Cu$K\alpha$). Powder neutron-diffraction data were collected at room temperature and 77 K on the HRPD angle-dispersive-type diffractometer installed on the JRR-3 reactor at the Japan Atomic Energy Research Institute (JAERI) (16). The incident neutron beam was monochromatized to give a wavelength of 1.823 Å using the 331 reflection of Ge. The HRPD has a bank of 64 counters placed at 2.5° intervals. The crystal structure of the sample was refined using the Rietveld method with the RIETAN 2000 program (17). The coherent scattering lengths used for refinement of the neutron-diffraction data were 8.24 fm for La, − 2.22 fm for ^{7}Li, − 3.438 fm for Ti, and 5.803 fm for O.

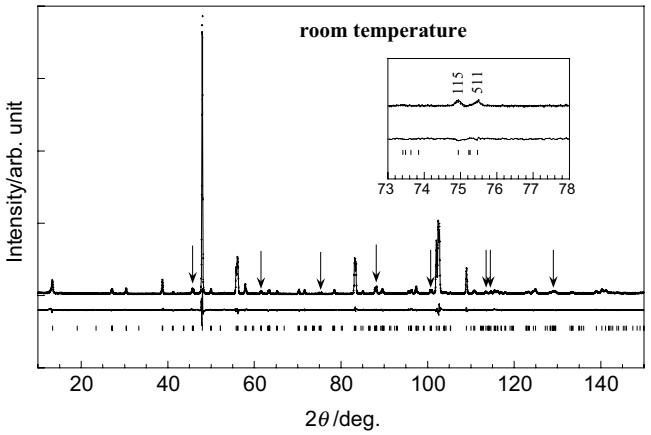

FIG. 1. Observed, calculated neutron-diffraction patterns, differences, and the peak position at room temperature for $La_{0.62}Li_{0.16}TiO_3$. Inset: part of the diffraction pattern. Arrows show extra peaks corresponding to the tilt of TiO_6 octahedra.

RESULTS AND DISCUSSION

The sample was confirmed to possess an orthorhombically distorted perovskite-structure by powder X-ray diffraction. The strong superlattice lines corresponding to the

TABLE 1
Structural Parameters in $La_{0.62}Li_{0.16}TiO_3$ at Room Temperature and 77 K

		Room temperature					77 K				
Site		g	x	y	z	B/Å^2	g	x	y	z	B/Å^2
La1	4*i*	0.939[a]	0	0.2525(8)	0	0.82(4)	0.939[a]	0	0.2523(7)	0	0.45(4)
La2	4*j*	0.301(4)[a]	0	0.255(2)	1/2	1.06(12)	0.301(4)[a]	0.0	0.255(2)	1/2	0.90(14)
Li1	8*n*	0.013[a]	0	0.311[b]	0.102[b]	6.4[c]	0.013[a]	0.0	0.283[b]	0.198[b]	3.7[c]
Li2	8*n*	0.147[a]	0	0.189(10)[b]	0.398(9)[b]	6.4(20)[c]	0.147[a]	0.0	0.217(8)[b]	0.302(6)[b]	3.7(12)[c]
Ti	8*o*	1	0.2484(15)	0	0.2599(4)	0.89(5)	1	0.2500(12)	0	0.2593(4)	0.64(5)
O1	4*g*	1	0.2720(8)	0	0	1.54(9)	1	0.2729(7)	0	0	1.27(8)
O2	4*k*	1	0	0	0.2142(6)	1.16(10)	1	0	0	0.2119(5)	0.98(9)
O3	4*l*	1	0	1/2	0.2595(6)	1.37(11)	1	0	1/2	0.2603(5)	0.95(9)
O4	8*m*	1	1/4	1/4	0.2345(5)	1.28(6)	1	1/4	1/4	0.2340(4)	1.09(6)
O5	4*h*	1	0.2319(8)	0	1/2	1.69(9)	1	0.2321(7)	0	1/2	1.30(8)
		a = 7.7313(1) Å, b = 7.7520(1) Å, c = 7.7840(1) Å R_{wp} = 8.79%, R_p = 6.55%, R_e = 4.44%, S = 1.98, R_I = 4.60%, R_F = 5.05%					a = 7.7224(1) Å, b = 7.7448(1) Å, c = 7.7735(1) Å R_{wp} = 8.78%, R_p = 6.55%, R_e = 4.34%, S = 2.02, R_I = 4.44%, R_F = 4.70%				

Note. Orthorhombic space group: *Cmmm* (No. 65), $Z = 8$.

[a] Occupancy for M atom $g(M)$ is constrained as follows: g(La1) = 1.24–g(La2), g(Li1) = 0.2106 g(La2) − 0.0506 and g(Li2) = 0.2106 {1 − g(La2)}.

[b] Position of Li is constrained as follows: y(Lil) = $\frac{1}{2} - y$(Li2) and z(Li1) = $\frac{1}{2} - z$(Li2).

[c] Thermal parameter B for Li is constrained as follows: B(Li1) = B(Li2).

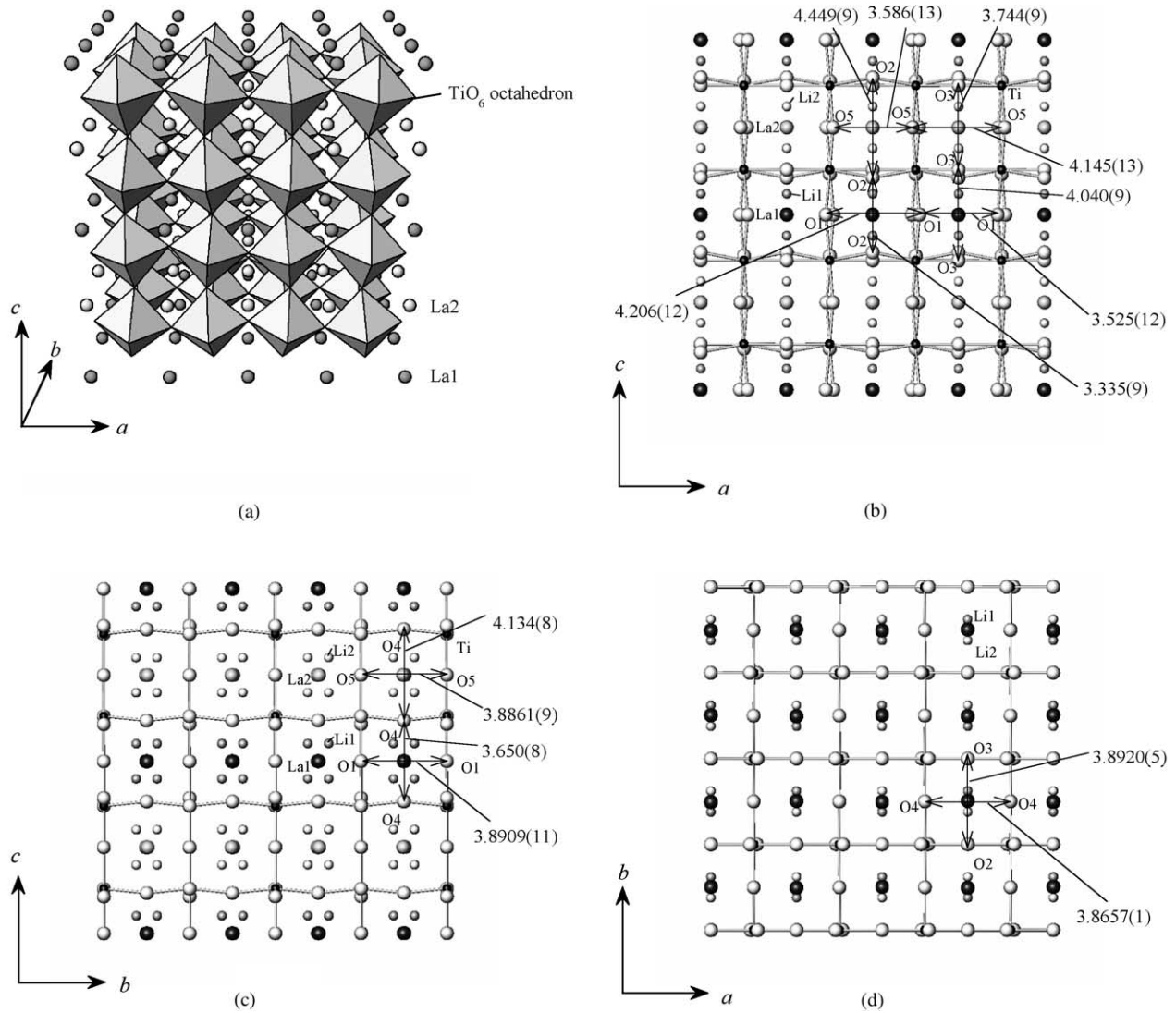

FIG. 2. Crystal structure of $La_{0.62}Li_{0.16}TiO_3$; (a) the structure from the perspective of the TiO_6 octahedral framework, (b) the *ca*, (c) *bc*, and (d) *ab* projections of structure at room temperature, respectively. The digits in the figures have the unit Å.

ordered arrangement of La ions that have been reported previously were also observed. ICP chemical analysis showed that the molar ratio of metals in the sample was $La:Li:Ti = 0.62 \pm 0.02 : 0.16 \pm 0.01 : 1$, resulting in the formula $La_{0.62(2)}Li_{0.16(1)}TiO_{3.01(3)}$. Here, the oxygen content was determined from the electroneutrality. The loss of Li with respect to a nominal amount was observed. This composition corresponds to that with $x = 0.05$ for $La_{2/3-x}Li_{3x}TiO_3$.

The powder neutron-diffraction pattern of $La_{0.62}Li_{0.16}TiO_3$ at room temperature is shown in Fig. 1. Because the neutron-diffraction pattern at 77 K is the same as that at room temperature, it can be concluded that no structural phase transition occurs in this temperature range. In addition to reflections that included the superlattice reflections corresponding to the alternative arrangement of La ions along the *c*-axis assigned to the orthorhombic cell with $a(\sim a_p) \times b(\sim a_p) \times c(\sim 2a_p)$ (space group: *Pmmm*) as previously reported, some extra reflections (indicated by arrows in Fig. 1) were also detected. All of these reflections can be indexed using a larger cell with $a(\sim 2a_p) \times b(\sim 2a_p) \times c(\sim 2a_p)$. The indices of additional superstructure reflections have the type: $2p+1\ \ 2q+1\ \ 2r+1$ (p, q and r are integers). When observing the X-ray diffraction pattern carefully, only one additional peak with very weak intensity corresponding to the index 311 can be detected, with other additional peaks being too weak to be detected.

The tilting of the oxygen octahedra in perovskites causes a doubling of the basic unit-cell axes, and extra reflections appear that lie on half-integral reciprocal planes. Glazer has described a simple technique for creating a trial model for the structure of perovskite (18, 19). According to Glazer, the tilt in anti-phase of oxygen octahedra gives rise to reflections of the type: $h + \frac{1}{2}\ k + \frac{1}{2}\ l + \frac{1}{2}$ (h, k and l are integers) with a basic perovskite cell, that is, $2p + 1\ 2q + 1\ 2r + 1$ (p, q and r are integers) with a double cell. Since the intensity of these reflections depends primarily on the scattering factor of oxygen, it is expected that the reflections have a weak intensity in the X-ray diffraction pattern, while they can be apparently detected in neutron diffraction. Therefore, the observed extra reflections are thought to be due to the tilt of TiO_6 octahedra. Furthermore, it was found that the extra reflections appear under the condition that $h = 2p + 1$, $k = 2q + 1$, $l = 2r + 1$ (p, q and r are integers) and $h \neq l$ when $a < b < c$. An example is shown in the inset of Fig. 1. Though 115 and 511 reflections were observed, a 151 reflection was not, suggesting that the anti-phase tilt of the TiO_6 octahedron occurs along the b-axis (Glazer's notation $a^0\ b^-\ c^0$). General reflection conditions were reduced as follows: $h + k = 2n$ and $h\,0\,l$ ($l = 2n + 1$) (n is an integer). The possible space groups are $C222$ (No. 21), $Cmm2$ (No. 35), $Cm2m$ ($Amm2$) (No. 35), $C2mb$ ($Abm2$) (No. 39), $Cmmm$ (No. 65), and $Cmma$ (No. 67). Of these, only two space groups, $Cm2m$ and $Cmmm$, permit the tilting model. $Cmmm$ with higher symmetry (point group: mmm) is one of the minimal supergroups of $Cm2m$ (point group: $mm2$). In this study, $Cmmm$ with higher symmetry was adopted, and a Rietveld refinement was carried out. Refinement of the Li position was first done using the data obtained at 77 K, as Li ions are less mobile at 77 K than at room temperature (20) and it is easy to determine the position at which they become stable. Here, supposing the Li ions distribute randomly among A-sites, constraints for the site occupancies of La and Li were determined, and the isotropic thermal parameter B of Li was common (Table 1). When the Li positions are the same as those of La, a higher B as high as 14 Å^2 even at 77 K is obtained, indicating that Li does not reside at the centre of the A-sites. This finding is supported by the results of Skakle *et al.* regarding $Li_{0.5-3y}Re_{0.5+y}TiO_3$ (Re = Pr, Nd; $y = 0.05$) (15), the simple energetic calculations (21) and molecular dynamics simulation of $La_{0.6}Li_{0.2}TiO_3$ (22). Therefore, the positions of Li were deviated from the center into two equivalent positions (Wycoff's notation 8n) with regard to an A-site, resulting in a lower B as high as 3.7 ± 1.2 Å^2. When Li ions were placed at general 16r position, the error of the x-coordinate was very large and on the order of 0.1. Consequently, Li ions were placed at the 8n position. The stable positions of Li at room temperature, which are thought to be similar to those at 77 K, were refined. The observed, calculated patterns, differences, and peak positions at room temperature for $La_{0.62}Li_{0.16}TiO_3$ are shown in Fig. 1. Table 1 lists the crystal data at room temperature and 77 K. The higher B value for Li at room temperature (6.4 ± 2.0 Å^2) than that at 77 K implies that Li ions are highly mobile. The site occupancies of La1 and La2 sites were found to be 0.94 and 0.30, respectively, implying that the ionic conduction in the La-poor layer (La1 layer) occurs more easily from the viewpoint of site percolation. Figure 2 shows the crystal structure of $La_{0.62}Li_{0.16}TiO_3$, and 2a shows the structure from the perspective of the octahedral framework. The structure contains a three-dimensional framework of corner-sharing TiO_6 octahedra that are tilted along the b-axis. Figures 2b, 2c, and 2d show the ca, bc, and ab projections of structure at room temperature, respectively. Table 2 lists the selected interatomic distance and the bond angles at room temperature and 77 K. At 77 K, Li ions are coordinated by four oxygen ions with Li–O lengths in the range 1.75–2.21 Å rather than six oxygen ions adding the two oxygen ions with longer Li–O lengths in the range 2.87–2.90 Å. These results are in good

TABLE 2
Selected Interatomic Distances (Å) and Bond Angles (°) for $La_{0.62}Li_{0.16}TiO_3$ at Room Temperature and 77 K

	Room temperature	77 K
La1–O1 (×2)	2.605(5)	2.599(4)
La1–O1 (×2)	2.873(5)	2.874(4)
La1–O2 (×2)	2.571(5)	2.556(5)
La1–O3 (×2)	2.786(5)	2.788(4)
La1–O4 (×4)	2.659(3)	2.652(2)
La2–O2 (×2)	2.974(13)	2.988(11)
La2–O3 (×2)	2.669(14)	2.657(12)
La2–O4 (×4)	2.830(3)	2.829(3)
La2–O5 (×2)	2.667(13)	2.669(12)
La2–O5 (×2)	2.813(12)	2.806(11)
Li1–O1 (×2)	2.43(6)	2.87(4)
Li1–O2	2.56(7)	2.19(6)
Li1–O3	1.91(9)	1.75(6)
Li1–O4 (×2)	2.24(5)	1.968(15)
Li2–O2	2.05(7)	1.82(6)
Li2–O3	2.64(9)	2.21(6)
Li2–O4 (×2)	2.36(5)	2.019(15)
Li2–O5 (×2)	2.45(6)	2.90(4)
Ti–O1	2.031(3)	2.024(3)
Ti–O2	1.953(11)	1.965(10)
Ti–O3	1.945(11)	1.931(10)
Ti–O4 (×2)	1.9481(5)	1.9462(4)
Ti–O5	1.874(3)	1.876(3)
O1–Ti–O5	178.7(7)	179.2(6)
O2–Ti–O3	169.4(3)	169.4(2)
O4–Ti–O4	168.3(3)	168.4(2)
Ti–O1–Ti	169.7(7)	169.9(6)
Ti–O2–Ti	159.0(3)	158.4(3)
Ti–O3–Ti	179.8(3)	179.5(3)
Ti–O4–Ti	168.4(3)	168.4(2)
Ti–O5–Ti	172.2(8)	171.6(7)

TABLE 3
Interatomic Distances (Å) around the Bottle neck at Room Temperature and 77 K

	Room temperature	77 K
O1–O1	3.525(12)	3.507(10)
	3.8909(11)	3.8885(9)
	4.206(12)	4.215(10)
O2–O2	3.335(9)	3.295(8)
	4.449(9)	4.479(8)
O2–O3	3.8920(5)	3.8906(5)
O3–O3	3.744(9)	3.726(7)
	4.040(9)	4.047(7)
O4–O4	3.650(8)	3.638(7)
	3.8657(1)	3.8612(1)
	4.134(8)	4.136(7)
O5–O5	3.586(13)	3.585(11)
	3.8861(9)	3.8822(8)
	4.145(13)	4.138(11)

agreement with the Li–O lengths in the range 2.05–2.23 Å (Li coordination is distorted tetrahedral) for $Li_{0.5-3y}Re_{0.5+y}TiO_3$ (Re = Pr, Nd; $y = 0.05$) after Skakle *et al.* (15) and the Li–O length expected from the ionic radii after Shannon (Li(IV) 0.59 Å and O(VI) 1.40 Å (23)). Compared to 77 K, at room temperature the stable position of Li ions shifts against the centre of A-site in the *b*-direction and toward the center of A-site in the *c*-direction, having five- or six-fold coordination with the Li–O lengths in the range 1.91–2.64 Å rather than fourfold coordination.

According to a simple energetic calculation, Li ions enter an activated state in the sites between adjacent A-sites surrounded by four oxygens, called a "bottleneck" and the activation energy for ionic conduction is determined primarily by the repulsion energy due to these oxygens (21). Therefore, a decrease in the bottleneck size leads to an increase in the activation energy. The La-ordering and the tilt of TiO_6 octahedra produce various kinds of bottlenecks of various size. The interatomic distances between two oxygen atoms at the bottleneck are shown in Figs. 2b–2d and are listed in Table 3. Some are less than the 3.98 Å value expected for the ionic radius if supposing that the Li and O ions are in contact. As seen in Figs. 2b–2d and Table 3, the size of the bottleneck in the La(2) layer (La-poor layer) is larger, on average, than that in the La(1) layer (La-rich layer). In addition, the size of the bottleneck along the *a*-axis is largest in the La(2) layer (La-poor layer). These results imply that Li ions in the La(2) layer (La-poor layer) are more conductive than those in the La(1) layer (La-rich layer), and are most conductive along the *a*-axis in the La(2) layer in this compound.

CONCLUSIONS

The Rietveld refinement using neutron-diffraction data for one $La_{2/3-x}Li_{3x}TiO_3$ series, furnace-cooled $La_{0.62}Li_{0.16}TiO_3$, was carried out. The structure of this compound contains a three-dimensional framework of corner-sharing TiO_6 octahedra that are tilted along the *b*-axis, alternatively arranged La along the *c*-axis, and Li in two equivalent off-centered positions of the A-site. Though this compound has a three-dimensional structure, the ionic conduction is expected to occur two-dimensionally rather than three-dimensionally due to their structural features. It was found that the positional information for oxygen, including the tilt of BO_6 in the perovskite-type lithium ion conducting oxides, is indispensable for the elucidation of the conduction mechanism, in addition to information regarding the arrangement of A-site ions like La.

ACKNOWLEDGMENTS

We thank Dr. H. Ohno for arranging the neutron-diffraction experiment, and Mr. Y. Shimojo and the members of the JRR-3 Operation Division, Department of Research Reactor Operation, JAERI for their help with the neutron-diffraction experiment. We are grateful to the reviewers for their advice and comments. Part of this work was financially supported by "the Asahi Glass Foundation" and "Saneyoshi Scholarship Foundation."

REFERENCES

1. L. Latie, G. Villeneuve, D. Conte, and G. L. Flem, *J. Solid State Chem.* **51,** 293 (1984).
2. A. G. Belous, G. N. Novitsukaya, S. V. Polyanetsukaya, and Yu. I. Gornikov, *Izv. Akad. Nauk SSSR, Neorg. Mater.* **23,** 470 (1987); *Russ. J. Inorg. Chem.* **32,** 156 (1987). [translated from *Zh. Neorg. Khim.* **32,** 283 (1987)]
3. Y. Inaguma, L. Chen, M. Itoh, T. Nakamura, T. Uchida, H. Ikuta, and M. Wakihara, *Solid State Commun.* **86,** 689 (1993).
4. M. Abe and K. Uchino, *Mater. Res. Bull.* **9,** 147 (1974).
5. H. Kawai and J. Kuwano, *J. Electrochem. Soc.* **141,** L78 (1994).
6. A. D. Robertson, S. García-Martín, A. Coats, and A. R. West, *J. Mater. Chem.* **5,** 1405 (1995).
7. J. L. Fourquet, H. Duroy, and M. P. Crosnier-Lopez, *J. Solid State Chem.* **127,** 283 (1996).
8. A. I. Ruiz, M. L. López, M. L. Veiga, and C. Pico, *J. Solid State Chem.* **148,** 329 (1999).
9. J. Ibarra, A. Várez, C. León, J. Santamaría, L. M. Torres-Martínez, and J. Sanz, *Solid State Ionics* **134**, 219 (2000).
10. M. A. París, J. Sanz, C. León, J. Santamaría, J. Ibarra, and A. Várez, *Chem. Mater.* **12,** 1694 (2000).
11. A. Várez, F. García-Alvarado, E. Morán, and M. A. Alario-Franco, *J. Solid State Chem.* **118,** 78 (1995).
12. Y. Inaguma, T. Katsumata, J. Yu, and M. Itoh, *Mater. Res. Soc. Symp. Proc* **453,** 623 (1997).
13. Y. Inaguma and M. Itoh, *Solid State Ionics* **86–88,** 257 (1996).
14. Y. Harada, T. Ishigaki, H. Kawai, and J. Kuwano, *Solid State Ionics* **108,** 407 (1998).
15. J. M. S. Skakle, G. C. Mather, M. Morales, R. I. Smith, and A. R. West, *J. Mater. Chem.* **5,** 1807 (1995).

16. Y. Morii, K. Fuchizaki, S. Funahashi, N. Minakawa, Y. Shimojo, and A. Ishida, "Proccedings of the Fourth International Symposium on Advanced Nuclear Research, Mito, p. 280." 1992.
17. F. Izumi and T. Ikeda, *Mater. Sci. Forum* **321–324,** 198 (2000).
18. M. Glazer, *Acta Crystallogr. B* **28,** 3384 (1972).
19. M. Glazer, *Acta Crystallogr. A* **31,** 756 (1975).
20. M. Oguni, Y. Inaguma, M. Itoh, and T. Nakamura, *Solid State Commun.* **91,** 627 (1994).
21. Y. Inaguma, Y. Matsui, J. Yu, Y-J. Shan, T. Nakamura, and M. Itoh, *J. Phys. Chem. Solids* **58,** 843 (1997).
22. T. Katsumata, Y. Inaguma, M. Itoh, and K. Kawamura, *J. Ceram. Soc. Jpn.* **107,** 615 (1999).
23. R. D. Shannon, *Acta Crystallogr. A* **32,** 751 (1976).